Early Patellofemoral Cartilage and Bone Degeneration in a Rat Model of Noninvasive

Anterior Cruciate Ligament Rupture

[1]Samantha E. Hartner, MS; [1]Michael D. Newton, MS; [1]Mackenzie M. Fleischer, MS; [1,2]Kevin C.

Baker, PhD; [3]Tristan Maerz, PhD*

[1] Orthopaedic Research Laboratory, Beaumont Health, Royal Oak, MI

[2] Department of Orthopaedic Surgery, Oakland University – William Beaumont School of

Medicine, Rochester, MI

[3] Department of Orthopaedic Surgery, University of Michigan, Ann Arbor, MI

*Corresponding Author:

Tristan Maerz, PhD

Department of Orthopaedic Surgery, University of Michigan

109 Zina Pitcher Place, Ann Arbor MI 48109

Phone: 734 936 2566; E-Mail: tmaerz@umich.edu

Running Title: Patellofemoral OA after ACL Rupture

Author contributions

All authors have made substantial contributions to the conception and design of the study,

acquisition of data, and/or analysis and interpretation of data, as well as manuscript preparation

and final approval of the submitted manuscript. TM takes responsibility for the integrity of the

work as a whole. Investigation performed at the Orthopaedic Research Laboratories of Beaumont

Health in Royal Oak, Michigan.

24 **ABSTRACT**

25 **Background:** Anterior cruciate ligament rupture (ACLR) is a well-known risk factor for the

26 development of post-traumatic osteoarthritis (PTOA). While clinical and pre-clinical studies

27 have characterized the onset and progression of PTOA in the tibiofemoral joint compartment,

28 very little is known about degenerative changes in the patellofemoral compartment after ACL

29 injury.

30 **Hypothesis/Purpose:** To evaluate the extent to which ACL rupture induces acute patellofemoral

31 joint degeneration by quantifying articular cartilage morphology and remodeling of subchondral

32 and trabecular bone microarchitecture in the patellofemoral compartment.

33 **Study Design:** Descriptive laboratory study.

34 **Methods:** Adult female Lewis rats were randomized to undergo either a non-surgical ACL

35 rupture or a Sham procedure (n = 6 per group). *Ex vivo* contrast-enhanced micro-computed

36 tomography (µCT) and histological evaluation of the patellofemoral compartment were

37 performed at 2-weeks post-injury, representing a timepoint of documented early PTOA in the

38 tibiofemoral compartment in this model.

39 **Results:** ACL rupture causes osteophyte formation in the patella and mild degeneration in the

40 superficial zone of articular cartilage (AC), including surface fibrillation, fissures, increased

41 cellularity, and abnormal chondrocyte clustering at two weeks post-injury. Contrast-enhanced

42 µCT analysis demonstrates significant increases in AC thickness of patellar and trochlear

43 cartilage. Loss of subchondral bone thickness, bone volume fraction, and tissue mineral density,

44 as well as changes to trabecular microarchitecture in both the patella and trochlea, were

45 indicative of catabolic bone remodeling.

46   **Conclusion:** These results demonstrate that the patellofemoral joint develops mild but evident

47   degenerative changes in the acute time period following ACL rupture, extending the utility of

48   this rat model to the study of degenerative patellofemoral changes following joint trauma.

49   **Clinical Relevance:** ACL rupture causes mild degeneration and swelling of articular cartilage,

50   coupled with catabolic bone remodeling in the patellofemoral compartment. Characterizing the

51   pathophysiology of patellofemoral PTOA in its early stages may provide a better understanding

52   of disease progression and provide opportunities for preventative therapeutic intervention.

53

54   **Key Terms:** post-traumatic osteoarthritis; patellofemoral cartilage; bone microarchitecture;

55   anterior cruciate ligament rupture

56

INTRODUCTION

Anterior cruciate ligament (ACL) rupture is one of the most common soft-tissue musculoskeletal injuries and a well-known risk factor for post-traumatic osteoarthritis (PTOA)[4,24]. The progression of tibiofemoral PTOA following ACL rupture has been well-characterized in both clinical and pre-clinical literature[6,22,25,41]. However, comparatively few studies have characterized patellofemoral compartment OA (PFOA) following ACL rupture, and relatively little is known regarding incidence and overall phenotypic manifestation of joint degeneration in this compartment. Recent work suggests that PFOA may be equally or even more prevalent than tibiofemoral OA: Culvenor *et al* demonstrate that within 5-10 years post-ACL rupture, 47% of patients exhibit PFOA progression – including osteophytes, cartilage lesions, and joint space narrowing – compared to a 31% incidence of tibiofemoral OA[9]. Furthermore, recent MRI-based assessment of PFOA indicated that 40% of patients exhibit detectable patellofemoral cartilage loss within 5 years of ACL injury, with cartilage thickness in the trochlea decreasing by as much as 1% annually in the first 2 years[8].

Despite clinical evidence of a high incidence of PFOA development after ACL injury, the acute manifestations of PFOA and the associated microstructural, cellular, and molecular changes following ACL injury remain poorly understood. Clinical evidence regarding the nature of early patellofemoral tissue changes is lacking, as most clinical studies of PFOA track joint degeneration once disease has already developed. Natural history studies assessing PFOA incidence and development commonly employ radiography[9,20,32,34], which can diagnose joint space narrowing and osteophyte formation but is inherently incapable of assessing the extent and location of articular cartilage and bone degeneration, especially in early disease. While MRI is the gold-standard for assessment of cartilage thickness and bone marrow lesions[7,8,21], it lacks

80   imaging resolution to measure injury-induced changes to bone microarchitecture. Thus, the

81   collective understanding of acute PFOA following ACL injury is currently limited.

82   Small animal models of ACL injury have become invaluable tools for the preclinical

83   study of PTOA. In a previous rat study of surgical ACL transection, decreased subchondral bone

84   (SCB) perfusion and associated cartilage and bone lesions were observed in the patellofemoral

85   compartment at intermediate and chronic time points following injury[40], demonstrating chronic

86   manifestations of ACL injury in the rodent patellofemoral compartment. However, this study did

87   not analyze acute time points to understand early disease, and surgical models of ACL injury are

88   inherently limited in their assessment of acute injury due to the confounding influence of surgical

89   trauma and lack of mechanical loading. Non-invasive models of isolated ACL rupture, whereby

90   joint injury is induced mechanically, provide a highly controlled and clinically-representative

91   means of inducing joint injury, and the utilization of these models to study tibiofemoral PTOA

92   has increased in recent years[3,6,23,26,38]. However, to date, the extent of patellofemoral remodeling

93   and degeneration in these non-invasive injury models remains largely unexplored, and it is

94   unclear to what extent these models may be employed to study PFOA pathophysiology and

95   potential treatments. To this end, the aim of this study was to employ both quantitative imaging

96   and histological evaluation to characterize acute changes to bone and articular cartilage within

97   the patellofemoral joint in a rat model of non-invasive ACL rupture.

98

99   **MATERIALS AND METHODS**

100   *Rats and Non-Invasive ACL Rupture*

101   Under an IACUC-approved protocol, 12 female Lewis rats (aged 14 weeks, weight ~200-

102   220g, Charles River Laboratories, Wilmington, MA) were randomized to either non-invasive

5

103   ACL rupture (ACLR) or Sham groups (n = 6 per group). The sample size was determined based

104   on published μCT data from the same model[25]: given the previously-observed effect size in

105   trabecular bone volume fraction between control rats and ACLR rats (a morphometric parameter

106   most responsive to injury and an outcome we deemed most applicable to the present study) in

107   order to detect a 5% difference between groups, (effect size = 2.2, α = 0.05, power = 0.9), six rats

108   would be required. To induce ACLR or Sham injury, rats were placed prone on a materials

109   testing system (Insight 5, MTS, Eden Prairie, MN) with the right knee positioned in 100° of

110   flexion and the hindpaw held in 30° of dorsiflexion in a custom fixture. In the ACLR group,

111   ACL rupture was induced by applying a preload, ten preconditioning cycles, and a subsequent

112   rapid compressive displacement to the knee joint, as described previously[26]. The Sham group

113   was subjected to preload and preconditioning cycles only. Anesthesia was induced by

114   intraperitoneal ketamine and xylazine, and maintained under 1%-2% inhaled isoflurane. All rats

115   were administered 5 mg/kg subcutaneous carprofen immediately prior to Sham/ACLR injury,

116   and buprenorphine (1.2 mg/kg) was administered for analgesia at 12h and 24h post-procedure.

117   All procedures were completed in the morning, and rats individually housed and allowed *ad*

118   *libitum* cage activity and access to standard rodent chow under a 12-hour light/dark cycle for 2

119   weeks post-procedure until euthanasia via CO_2 asphyxiation. To perform contrast-enhanced

120   imaging, femora and patellae were completely dissected to expose the articular surface, fixed in

121   10% neutral buffered formalin for 48 hours, and transferred to 70% ethanol for long-term

122   storage.

123

124   *Ex Vivo Micro-Computed Tomography*

125   To facilitate contrast-enhanced µCT of articular cartilage, femora and patellae were

126   rehydrated in PBS overnight and incubated in 20% v/v ioxaglate (Hexabrix 320, Guerbet LLC,

127   Princeton, NJ) for 2 hours prior to µCT imaging as previously described[36]. In preliminary

128   experiments, a 2-hour contrast agent incubation was found to be sufficient to achieve equilibrium

129   in articular cartilage (data not shown). Both patellae and femora were securely positioned in

130   custom sample holders for consistent imaging positioning and orientation, and humidifying silica

131   beads were used to maintain a 70% humid environment during µCT acquisition. Femora were

132   scanned on a µCT-40 (Scanco Medical AG, Brüttisellen, Switzerland) at 55 kVp, 145 µA, 300

133   ms integration time, with an isotropic voxel size of 8 µm. Patellae were scanned on a VivaCT-80

134   (Scanco Medical AG) at 55 kVp, 145 µA, 800 ms integration time, with a 12 µm isotropic voxel

135   size. The use of two imaging systems was necessary given study timeline restrictions, and

136   validation data demonstrates equivalent morphometry results between these two imaging

137   resolutions (data not shown). Furthermore, no comparisons are made between the two imaging

138   protocols. Following scanning, specimens were washed in PBS for 30 minutes and graded back

139   to 70% ethanol.

140

141   *Imaging Analysis*

142   Femoral and patellar articular cartilage, subchondral bone, and trabecular bone volumes

143   of interest were isolated using an automated, atlas registration-based segmentation algorithm in

144   MATLAB (Mathworks, Natick, MA), as previously described[33]. All segmentations were

145   reviewed for accuracy by an experienced investigator. Femoral AC and bone volumes were

146   further segmented to isolate the trochlear compartment, defined as all bone and AC proximal to

147   the femoral notch. AC was quantitatively analyzed via mean thickness (AC.Th) using the direct-

148   distance transform (i.e "sphere-fitting") method in boneJ[11]. Trabecular bone was assessed via

149   bone volume fraction (BV/TV), tissue mineral density (TMD), trabecular thickness (Tb.Th),

150   trabecular spacing (Tb.Sp), and trabecular number (Tb.N) according to standard methods[2].

151   Subchondral bone was assessed via subchondral bone thickness (SCB.Th), BV/TV, and TMD. A

152   standardized hydroxyapatite phantom was used to calibrate imaging data to mineral density.

153

154   *Histology*

155   Patellae, including the attached quadriceps and patellar tendons, were decalcified,

156   embedded in paraffin and bisected sagittally, and a single 5 µm sagittal section (including both

157   halves) was taken. Femora underwent additional histological assessments of the femoral

158   condyles as part of a separate study on the tibiofemoral compartment which required the use of

159   non-decalcified methods[28]. As such, femora were embedded in methyl methacrylate and bisected

160   into medial and lateral halves. Two 5 µm sections were taken, spaced 200 µm apart. For this

161   study, trochlear analysis was carried out on lateral compartment sections, which fully

162   encompassed the trochlear articular cartilage. All sections of both patellae and femora were

163   stained with Safranin-O/Fast Green and imaged at 20x magnification using a slide imaging

164   system (Aperio, Leica 122 Biosystems, Buffalo Grove, IL). Two blinded raters scored each

165   section using the Osteoarthritis Research Society International (OARSI) Modified Mankin

166   score[16], and graders conferred on disparate scores (differences of greater than one point) until

167   consensus was reached. Histologic scores were averaged across all sections for each limb, and an

168   aggregate group average was calculated.

169

170   *Statistical Analyses*

171   Statistical analysis was performed using SPSS (IBM, Armonk, NY). The normality and

172   equal variance assumptions were confirmed for continuous data. μCT data were assessed via

173   mixed two-way analysis of variance (ANOVA) with one within-subject factor (Injured vs

174   Contralateral) and one between-subject factor (ACLR vs Sham). Histologic grades were assessed

175   via the Kruskal Wallis test, with *post hoc* comparisons via Mann-Whitney U tests with a

176   Bonferroni correction for multiple comparisons. Adjusted P values below 0.05 were considered

177   significant.

178

179   **RESULTS**

180   All animals maintained good health status for the 2-week period following the ACLR and

181   Sham procedures and thus all 6 rats from both experimental groups were included in the analysis.

182

183   *Articular Cartilage Exhibits Acute Swelling Following ACLR*

184   AC was significantly thicker in the ACLR Injured limb compared to the Contralateral

185   limb in the patella and trochlea (Patella – 12.3% increase, $P = 0.003$; Trochlea – 8.7% increase,

186     $P = 0.005$), and compared to the Sham Uninjured limb in the patella (18.8% increase, $P = 0.001$)

187   (**Figure 1**). Interestingly, patellar AC of the Sham Uninjured limb was significantly thinner

188   compared to the Sham Contralateral (8.1% decrease, $P = 0.026$), indicating a subtle effect of

189   sham loading. In the patella of the ACLR Injured limb, AC thickening occurred over the entire

190   superior cartilage surface, encompassing both the medial and lateral regions, while in the Sham

191   Uninjured limb, cartilage thinning was most pronounced on the superior and lateral surfaces

192   (**Figure 1A**). In the trochlea of the ACLR Injured limb, AC thickening occurred primarily in the

193   proximal aspect but with reduced magnitude compared to the patella (Trochlea: 8.7% increase;

9

194   Patella: 12.3% increase). Taken together, these findings demonstrate that ACLR induces acute

195   swelling/thickening of both patellar and trochlear articular cartilage, with a greater magnitude of

196   change observed in the patella.

197

198   *Injury-Induced Loss of Trabecular and Subchondral Bone is Observed in the Patella and*

199   *Trochlea*

200   ACLR induced catabolic trabecular and subchondral bone remodeling of both the patella

201   and the trochlea. In the patella, trabecular BV/TV, TMD, Tb.Th, and Tb.N were significantly

202   decreased and Tb.Sp was significantly increased in the ACLR Injured limb compared to the

203   Contralateral limb (BV/TV: 12.9% decrease, $P < 0.001$, TMD: 2.3% decrease, $P = 0.001$, Tb.Th:

204   6.8% decrease, $P < 0.001$, Tb.N: 6.5% decrease, $P < 0.001$, Tb.Sp: 10.1% increase, $P < 0.001$)

205   and compared to the Sham Uninjured limb (BV/TV: 12.7% decrease, $P < 0.001$, TMD: 2.0%

206   decrease, $P = 0.046$, Tb.Th: 6.4% decrease, $P = 0.022$, Tb.N: 6.8% decrease, $P = 0.001$, Tb.Sp:

207   10.8% increase, $P < 0.001$) (**Figure 2**). In the trochlea, epiphyseal Tb.Th was significantly

208   decreased in the ACLR Injured limb compared to both the Contralateral (4.3% decrease, $P =$

209   0.008) and Sham Uninjured limbs (6.2% decrease, $P = 0.002$). Epiphyseal BV/TV was

210   significantly lower in the ACLR Injured limb compared to the Sham Uninjured limb (7.3%

211   decrease, $P = 0.023$). In the subchondral compartment, subchondral BV/TV and thickness were

212   significantly decreased in the ACLR Injured limb compared to the Contralateral limb (Patella -

213   BV/TV: 3.6% decrease, $P = 0.001$, SCB.Th: 12.0% decrease, $P < 0.001$; Trochlea - BV/TV:

214   2.5% decrease, $P < 0.001$, SCB.Th: 11.5% decrease, $P < 0.001$) and compared to the Sham

215   Uninjured limb (Patella - BV/TV: 4.2% decrease, $P < 0.001$, SCB.Th: 15.0% decrease, $P =$

216   0.002; Trochlea - BV/TV: 2.9% decrease, $P = 0.002$, SCB.Th: 15.7% decrease, $P = 0.001$)

217   (**Figure 2**). Although no formal region-dependent analysis was performed, loss of SCB.Th

218   appeared to occur globally across the patella and trochlea in the ACLR limb, while in the Sham

219   limb, increased SCB.Th appears more pronounced on the inferior patella and medial trochlea.

220   Patellar SCB TMD was significantly decreased in the ACLR Injured limb compared to the

221   Contralateral limb (3.0% decrease, $P < 0.001$). SCB.Th of the Sham Uninjured limb was

222   significantly higher compared to the Sham Contralateral limb (Patella: 5.1% increase, $P = 0.014$,

223   Trochlea: 5.6% increase, $P = 0.010$). Taken together, these results demonstrate the acute loss of

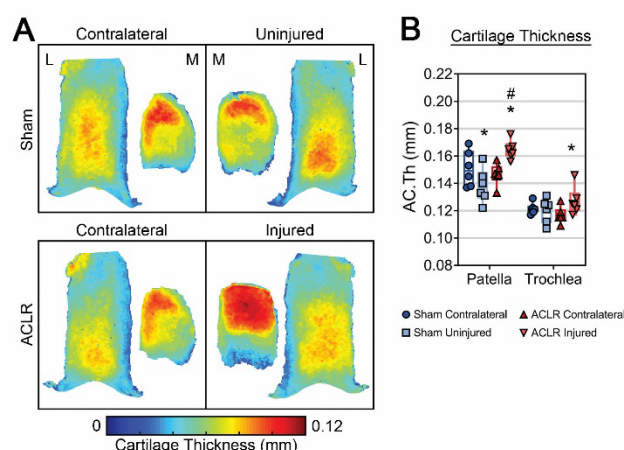224   both trabecular and subchondral bone in the patellofemoral compartment following ACLR.

225

226   **Figure 1.** *Three-dimensional articular cartilage thickness maps (A) and numerical thickness*

227   *results (B) derived from contrast-enhanced μCT demonstrate thickening of both patellar and*

228   *trochlear cartilage following ACLR. The top of the figure represents the superior/proximal*

229   *aspect of the patella and trochlea. n = 6 for all groups. * represents significant difference*

230   *compared to Contralateral limb (*$^{*}P < 0.05$, $^{**}P < 0.001$*); # represents significant difference*

231   *compared to Sham Uninjured limb (*$^{\#}P < 0.05$, $^{\#\#}P < 0.001$*); mixed two-way ANOVA.*
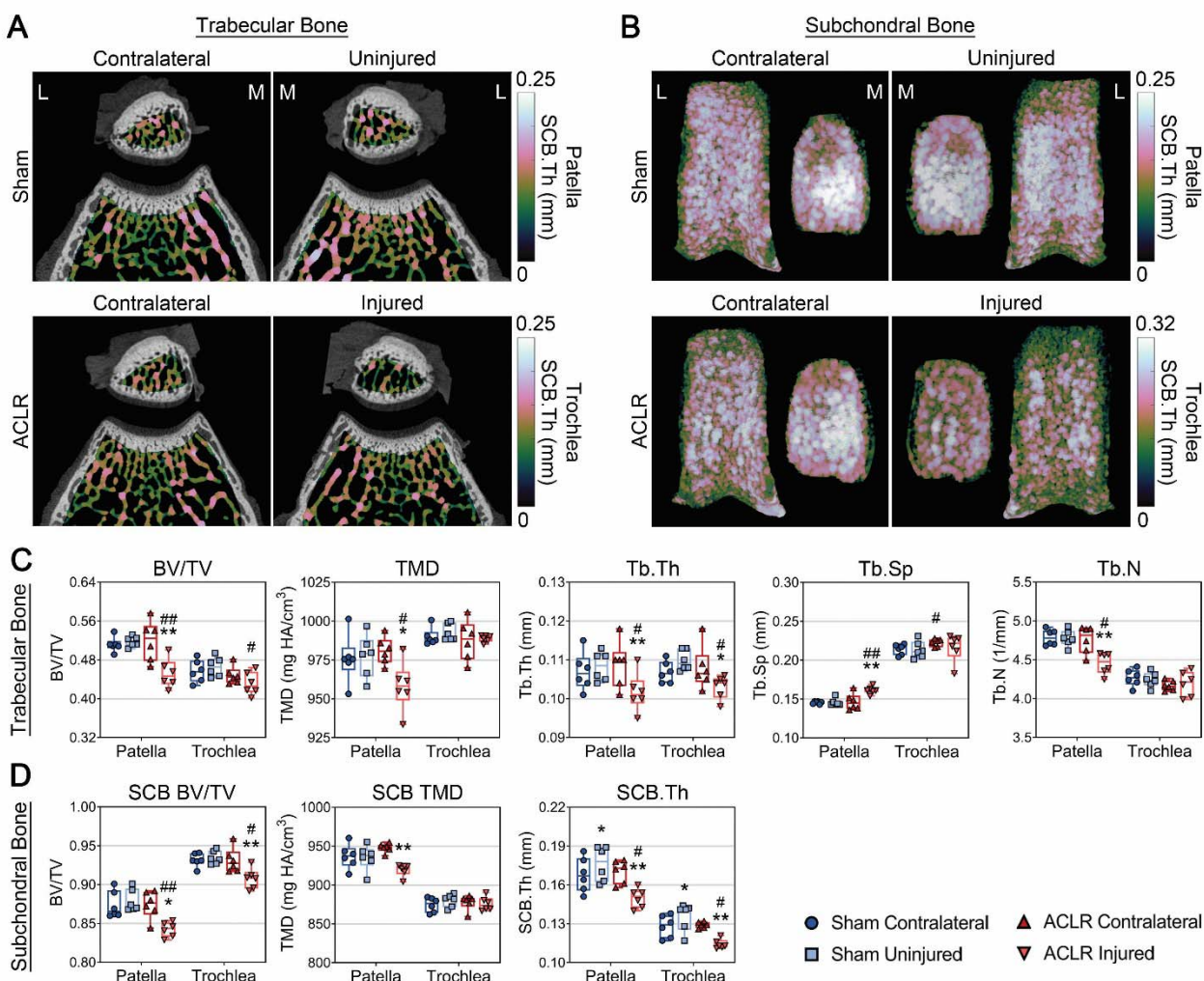
11

Figure 2. *Trabecular bone thickness maps of the patella and trochlea overlaid onto*

representative axial µCT images show increased Tb.Sp and reduced Tb.Th and Tb.N in the

ACLR Injured limb (A). 3D thickness maps show reduced subchondral bone thickness in the

patella and trochlea (B). Morphometric results demonstrate catabolic remodeling of both

trabecular (C) and subchondral bone (D) following ACL rupture. The overall magnitude of

catabolic remodeling was greater in the patella compared to the trochlea. The top of the figure

in B represents the superior/proximal aspect of the patella and trochlea. n = 6 for all groups. *

represents significant difference compared to Contralateral limb ($^{*}P < 0.05$, $^{**}P < 0.001$); $^{\#}$

241   *represents significant difference compared to Sham Uninjured limb ([#]P < 0.05, [##]P < 0.001);*

242   *mixed two-way ANOVA.*

243

244   *Histology Demonstrates Superficial Articular Cartilage Damage, Osteophyte Formation, and*

245   *Abnormal Chondrocyte Morphology Following ACL Rupture*

246   Patellar and trochlear cartilage of both Sham limbs appeared normal, with a smooth

247   articular surface, normal chondrocyte morphology, and homogenous Saf-O staining distributions.

248   While our contrast-enhanced μCT results demonstrate mild thinning of Sham Uninjured cartilage

249   in the patella, we did not observe any notable degenerative changes in Sham limbs on histology.

250   ACLR Injured patellae demonstrate mild but evident degenerative histological changes,

251   including surface fibrillation, reduction of intracellular and extracellular PG staining, increased

252   chondrocyte clustering, and osteophyte formation (**Figure 3A-B**). We also observed an increased

253   incidence of hypertrophic chondrocytes in deep cartilage, most notably at the superior patellar

254   aspect where articular cartilage thickening was observed. In superficial patellar cartilage, a

255   greater incidence of abnormal chondrocyte clustering was noted in ACLR Injured limbs (**Figure**

256   **3A, red arrowheads**). Superficial fissures and abnormal chondrocyte clustering were noted to be

257   more prevalent in the inferior region of patellar cartilage. Osteophytes appeared immature, with

258   primarily cartilaginous composition and focal regions of mineralized tissue, indicative of active

259   osteophyte formation. This osteophyte formation was exclusively observed at the superior aspect

260   of the patella (**Figure 3B**). Correspondingly, ACLR Injured patellae had a significantly higher

261   OARSI score compared to both ACLR Contralateral ($P = 0.015$) and Sham Uninjured limbs ($P =$

262   0.015), as well as several significantly higher sub-scores compared to both Contralateral (AC

263   Structure: $P = 0.018$, PG Staining: $P = 0.014$, Cellularity: $P = 0.008$, Osteophyte: $P = 0.004$) and

264   Sham Uninjured limbs (AC Structure: $P = 0.014$, PG Staining: $P = 0.014$, Cellularity: $P = 0.007$,

265   Osteophyte: $P = 0.004$) (**Figure 3C**).

266   ACLR Injured trochleae had largely intact cartilage surfaces, with only minor noted

267   superficial fibrillation (**Figure 4A, green arrowhead**). Notably, ACLR trochleae exhibited focal

268   regions of intense Saf-O staining and pockets of abnormal clustering/cloning in superficial-layer

269   cells. ACLR Injured trochleae had a significantly higher OARSI score compared to Sham

270   Uninjured limbs ($P = 0.024$). Multiple OARSI sub-scores were significantly higher in ACLR

271   trochleae compared to Sham Uninjured limbs (AC Structure: $P = 0.038$, PG Staining: $P = 0.022$,

272   Cellularity: $P = 0.023$) and the tidemark sub-score was significantly higher compared to ACLR

273   Contralateral limbs ($P = 0.035$) (**Figure 4B**). Taken together, our histologic results demonstrate

274   that at this acute post-injury timepoint, ACL rupture induces mild articular cartilage degeneration

275   of the patella and trochlea, largely contained to the superficial zone, and osteophyte formation at
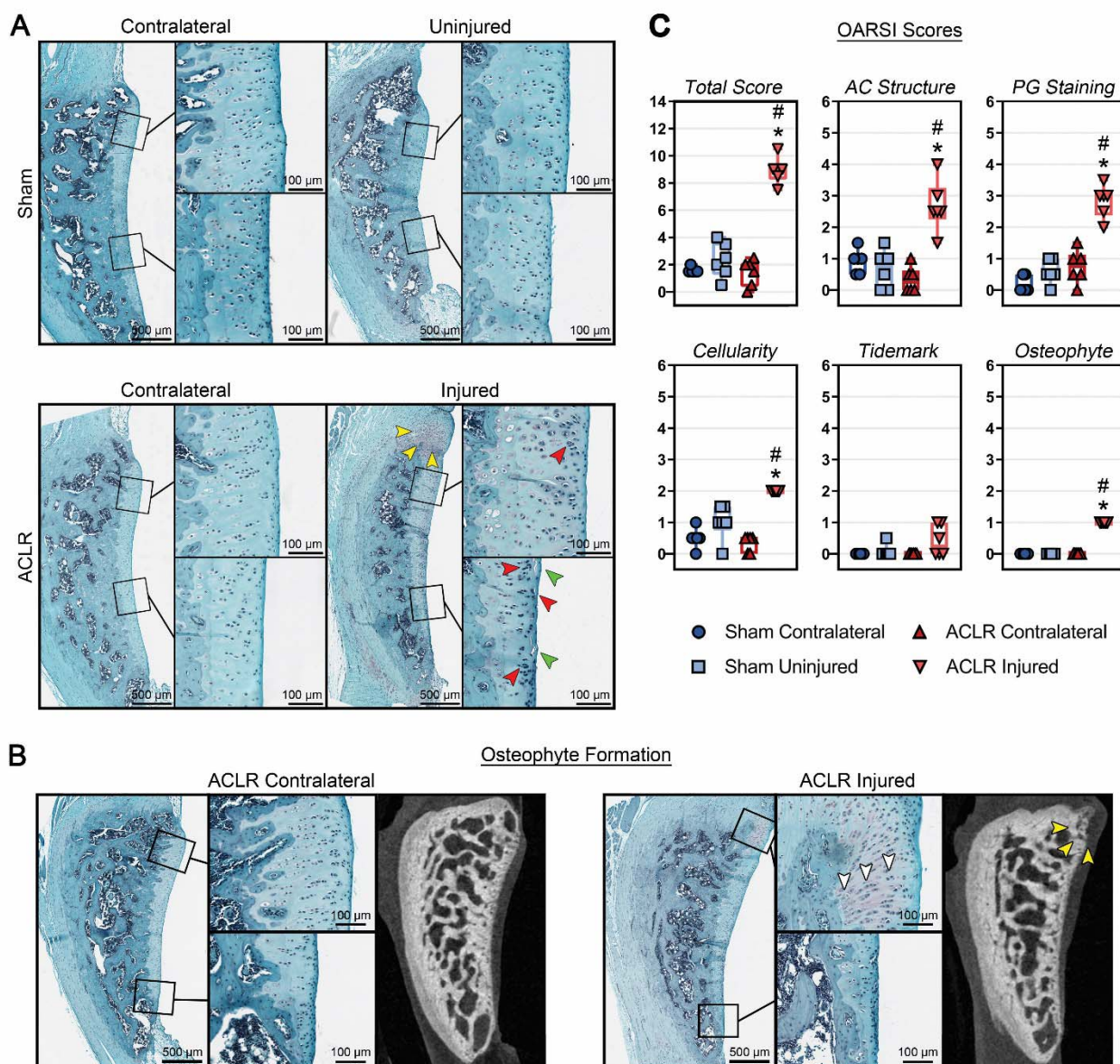
276   the superior aspect of the patella.

Figure 3. *Representative sagittal histology of patellae demonstrates that ACLR Injured patellae*

exhibit superficial fissures (green arrowheads), osteophyte formation (yellow arrowheads), and

abnormal chondrocyte morphology and clustering (red arrowheads) (A). Osteophyte formation

at the superior aspect of ACLR Injured patellae was evident on both histology and μCT.

Proliferation of hypertrophic and pre-hypertrophic chondrocytes indicative of endochondral

ossification is evident in superior aspect of the ACLR Injured patella (white arrowheads) (B).

ACLR Injured patellae exhibited significantly higher OARSI Modified Mankin scores and sub-

15

285   *scores compared to both ACLR Contralateral and Sham Uninjured patellae (Maximum OARSI*

286   *scores: Total Score – 21; AC Structure – 8; PG Staining – 6; Cellularity – 3; Tidemark – 1;*

287   *Osteophyte – 3) (C). The top of the figure represents the superior/proximal aspect of the patella.*

288   *n = 6 for all groups. * represents significant difference compared to Contralateral limb (P <*

289   *0.05); # represents significant difference compared to Sham Uninjured limb (P < 0.05); Kruskal-*
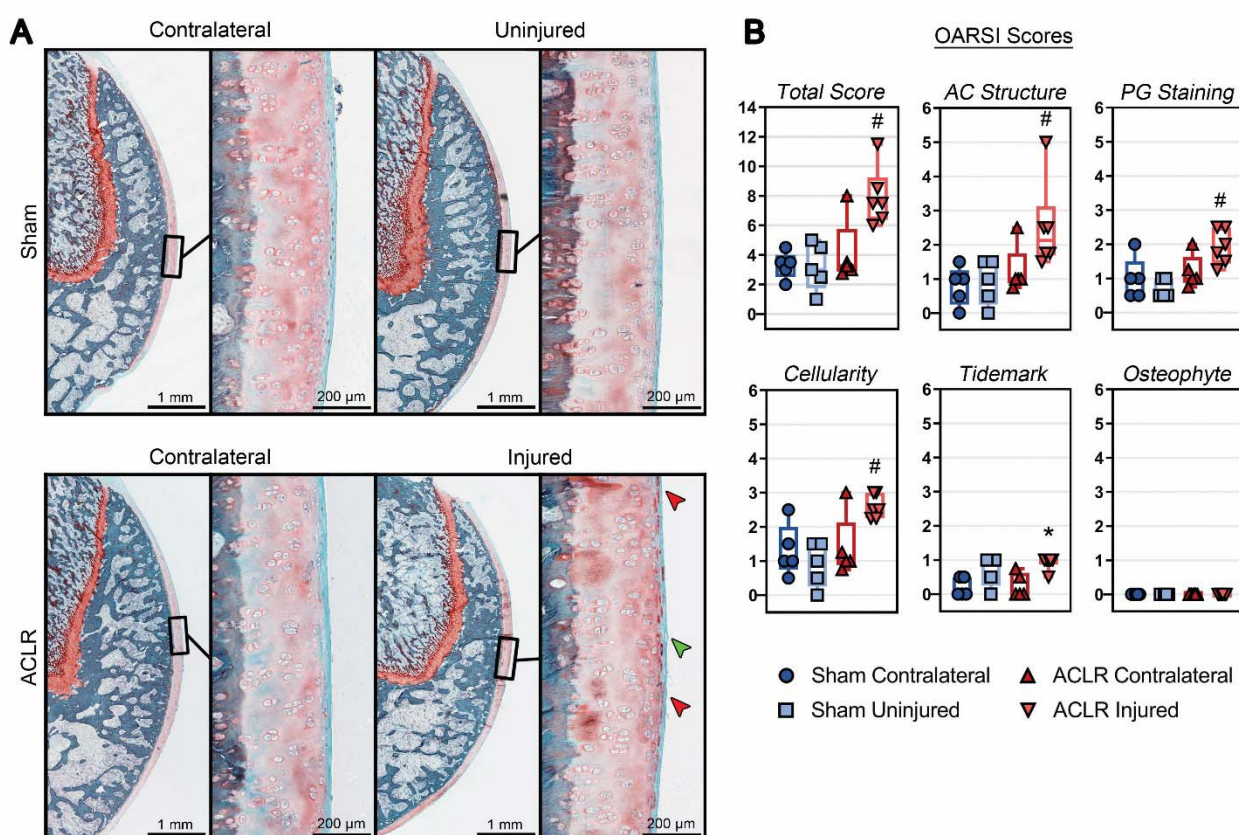
290   *Wallis ANOVA.*

291

Figure 4. *Representative sagittal trochlea histology shows that ACLR Injured patellae exhibit*

mild superficial fissures (green arrowhead), and abnormal chondrocyte morphology, clustering,

and focal regions of intense PG staining (red arrowheads) (A). ACLR Injured trochleae exhibit

significantly higher OARSI Modified Mankin scores and sub-scores compared to Sham

Uninjured trochleae (Maximum OARSI scores: Total Score – 21; AC Structure – 8; PG Staining

16

297   *– 6; Cellularity – 3; Tidemark – 1; Osteophyte – 3) (B). The top of the figure represents the*

298   *superior/proximal aspect of the trochlea. n = 6 for all groups. * represents significant difference*

299   *compared to Contralateral limb (P < 0.05);* [#] *represents significant difference compared to*

300   *Sham Uninjured limb (P < 0.05); Kruskal-Wallis ANOVA.*

301

302   **DISCUSSION**

303   Significant articular cartilage and subchondral bone remodeling in the weight-bearing

304   regions of the tibiofemoral compartment are the hallmarks of PTOA in the knee joint. However,

305   comparatively little is known about the development and progression of PTOA in the

306   patellofemoral compartment following ACL injury, or how PFOA contributes to overall disease

307   progression in the knee joint. In this study we aimed to characterize the onset of patellofemoral

308   cartilage and bone degeneration in a rat model of non-invasive ACL rupture, in which changes to

309   the patellofemoral compartment have not been characterized to date. Our results demonstrate

310   catabolic bone remodeling in both subchondral and trabecular bone, in addition to articular

311   cartilage swelling, abnormal changes to chondrocyte morphology and clustering, patellar

312   osteophyte formation, and surface degeneration of articular cartilage. Collectively, these findings

313   support that ACL rupture induces early patellofemoral compartment degeneration in this rat

314   model.

315   At 2 weeks following ACLR, quantitative μCT revealed significant thickening/swelling

316   of the articular cartilage in both the patella and trochlea while histological assessment showed

317   signs of superficial damage including surface fibrillation and fissuring. We observed an

318   increased incidence of hypertrophic chondrocytes in the deep AC layer of injured joints, which

319   qualitatively co-localized with regions of AC thickening observed in μCT. Taken together, these

17

320 manifestations are indicative of early cartilage disease. Studies in both humans and animal

321 models have shown that PTOA-associated AC degeneration initiates in the superficial zone with

322 the development of surface irregularities, fissures, and disruption of the superficial collagen

323 matrix[17,18,39]. Regarding cartilage thickness changes in response to injury, while some clinical

324 studies of PTOA with early MRI assessment report compartment-specific regions of AC

325 thickening[14,27,29], other studies report short-term cartilage thickness loss that often persists into

326 chronic disease[8,13,37]. Previous studies of ACL rupture in rats have reported AC thickening in the

327 tibial plateau, femoral condyles, and trochlea persisting for up to 10 weeks post-injury[29], but to

328 our knowledge this is the first study to report acute AC thickening in the patella using high-

329 resolution μCT. In contrast to our findings, a recent study employing ACL transection in rats

330 reported that both patellar and trochlear AC were histologically intact at 16 weeks post-injury,

331 with surface degeneration and hypertrophic chondrocytes presenting by 32 weeks[40]. While this

332 may reflect inherent differences between surgical vs non-invasive ACL injury, our findings of

333 early/mild cartilage damage underscore the value of high-resolution μCT in measuring the initial

334 cartilage response to traumatic injury, which may be undetected and cannot be comprehensively

335 quantified using histology or lower-resolution imaging modalities.

336 Acute loss of bone mineral density and bone volume following ACL rupture have been

337 well-described in clinical literature[22,41]. Both clinical and pre-clinical studies have found that in

338 the short term following ACL injury, subchondral and trabecular bone undergo catabolic

339 degeneration, followed by a transition toward anabolic remodeling. In the subchondral bone, this

340 remodeling persists in the long term, leading to subchondral bone sclerosis[1,6,21]. While animal

341 models have accurately characterized this remodeling using high-resolution imaging, the exact

342 nature of injury-induced catabolic bone remodeling in humans remains undescribed given that, to

18

343   date, there have been very few clinical studies employing high-resolution imaging capable of

344   accurately measuring bone microarchitecture. Recently, however, Kroker *et al* used HR-pQCT to

345   demonstrate that femoral subchondral bone thickness and BMD decreases for 7-8 months post-

346   ACL injury before entering a plateau or recovery phase[21]. The subchondral and trabecular bone

347   results of the current study share key similarities with this clinical work, affirming that at 2-

348   weeks following ACLR, distinct bone remodeling-related indicators of early PFOA are readily

349   observable in this rat model.

350   A notable finding in our dataset is that several injury-induced changes occurred with

351   greater magnitude in the patella compared to changes in the trochlea. While a few prior clinical

352   studies have reported more severe cartilage loss in the patella compared to the femoral

353   condyles[37] and trochlea[35], at least one other study has found that greater cartilage degeneration

354   occurs in the trochlea in the 2-5 year post-injury time period[8]. Thus, it remains unclear to what

355   extent this finding is specific to this animal model or specific to a stage of PTOA severity, and it

356   is beyond the scope of the current study to investigate the cause of this difference. However,

357   previous clinical research has demonstrated that compared to the other articular surfaces of the

358   knee, patellar AC uniquely exhibits a differential compressive strain response to variations in

359   physical activity and intensity level, suggesting that the patella may be more sensitive to

360   mechanical stimuli and instability than the trochlea[12,35]. This is consistent with cadaveric

361   findings that patellar AC has higher fluid permeability and lower proteoglycan content than

362   femoral AC, potentially making the patella more susceptible to mechanically-induced

363   degeneration[15]. It is also possible that the mechanism of injury used in our model places a load

364   on the patella during compression and subluxation of the tibia. Given the location of the patella

365   relative to the trochlea in 100º of flexion, this compression could be inducing some mild

366   degeneration in the patella while having a lesser effect on the trochlea. Future studies may assess

367   biomechanical and molecular mechanisms underpinning differential disease severity in the two

368   surfaces of the patellofemoral compartment.

369   Some limitations should be taken into consideration when interpreting the results of this

370   study. Although the Sham loading procedure did not cause any macroscopic injury or

371   histologically-observable degeneration, it did have measurable effects on the AC and

372   subchondral bone of the Sham limb compared to its contralateral. Sham effects are frequently

373   reported in other models of rodent ACL injury, including patellar tendon ossification, increased

374   AC water content, synovitis, and mild loss of proteoglycan at the AC surface resulting from a

375   sham surgical procedure[5,19,30,31]. The non-invasive Sham procedure described here may have

376   benefits over a surgical procedure involving skin and muscle incision and arthrotomy, which

377   could introduce multiple biological confounding effects. Finally, due to the differences in

378   histological processing and μCT scanning protocols used for the patella and the femur, we did

379   not make any direct comparisons between the patella and trochlea.

380   In this rat model of non-invasive ACL rupture, we observed acute degeneration of the

381   patellofemoral compartment, characterized by cartilage thickening and mild articular surface

382   damage alongside catabolic trabecular and subchondral bone remodeling. Injury-induced

383   changes in articular cartilage and trabecular bone were of greater severity in the patella than

384   changes in the trochlea. These results demonstrate the acute onset of mild patellofemoral joint

385   degeneration following ACL rupture and extend the utility of this rat joint injury model to the

386   study of patellofemoral PTOA.

387

388

20

REFERENCES

1.	Anderson DD, Chubinskaya S, Guilak F, et al. Post-traumatic osteoarthritis: improved understanding and opportunities for early intervention. J Orthop Res. 2011;29(6):802-809.

2.	Bouxsein ML, Boyd SK, Christiansen BA, et al. Guidelines for assessment of bone microstructure in rodents using micro-computed tomography. J Bone Miner Res. 2010;25(7):1468-1486.

3.	Brown SB, Hornyak JA, Jungels RR, et al. Characterization of Post□Traumatic Osteoarthritis in Rats Following Anterior Cruciate Ligament Rupture by Non□Invasive Knee Injury (NIKI). J Orthop Res. 2019.

4.	Carbone A, Rodeo S. Review of current understanding of post-traumatic osteoarthritis resulting from sports injuries. J Orthop Res. 2017;35(3):397-405.

5.	Chou M-C, Tsai P-H, Huang G-S, et al. Correlation between the MR T2 value at 4.7 T and relative water content in articular cartilage in experimental osteoarthritis induced by ACL transection. Osteoarthritis Cartilage. 2009;17(4):441-447.

6.	Christiansen BA, Anderson MJ, Lee CA, et al. Musculoskeletal changes following non-invasive knee injury using a novel mouse model of post-traumatic osteoarthritis. Osteoarthritis Cartilage. 2012;20(7):773-782.

7.	Culvenor AG, Collins NJ, Guermazi A, et al. Early Patellofemoral Osteoarthritis Features One Year After Anterior Cruciate Ligament Reconstruction: Symptoms and Quality of Life at Three Years. Arthritis Care Res (Hoboken). 2016;68(6):784-792.

8.	Culvenor AG, Eckstein F, Wirth W, Lohmander LS, Frobell R. Loss of patellofemoral cartilage thickness over 5 years following ACL injury depends on the initial treatment strategy: results from the KANON trial. Br J Sports Med. 2019;53(18):1168-1173.

9.	Culvenor AG, Lai CC, Gabbe BJ, et al. Patellofemoral osteoarthritis is prevalent and associated with worse symptoms and function after hamstring tendon autograft ACL reconstruction. Br J Sports Med. 2014;48(6):435-439.

10.	Culvenor AG, Segal NA, Guermazi A, et al. Sex□Specific influence of quadriceps weakness on worsening Patellofemoral and Tibiofemoral cartilage damage: a prospective cohort study. Arthritis Care Res. 2019;71(10):1360-1365.

11.	Doube M, Kłosowski MM, Arganda-Carreras I, et al. BoneJ: free and extensible bone image analysis in ImageJ. Bone. 2010;47(6):1076-1079.

12.	Eckstein F, Lemberger B, Gratzke C, et al. In vivo cartilage deformation after different types of activity and its dependence on physical training status. Ann Rheum Dis. 2005;64(2):291-295.

13.	Eckstein F, Maschek S, Wirth W, et al. One year change of knee cartilage morphology in the first release of participants from the Osteoarthritis Initiative progression subcohort: association with sex, body mass index, symptoms and radiographic osteoarthritis status. Ann Rheum Dis. 2009;68(5):674-679.

14.	Frobell RB. Change in cartilage thickness, posttraumatic bone marrow lesions, and joint fluid volumes after acute ACL disruption: a two-year prospective MRI study of sixty-one subjects. J Bone Joint Surg Am. 2011;93(12):1096-1103.

427   15.   Froimson MI, Ratcliffe A, Gardner TR, Mow VC. Differences in patellofemoral joint cartilage
428   material properties and their significance to the etiology of cartilage surface fibrillation. Osteoarthritis
429   Cartilage. 1997;5(6):377-386.

430   16.   Gerwin N, Bendele A, Glasson S, Carlson CS. The OARSI histopathology initiative–
431   recommendations for histological assessments of osteoarthritis in the rat. Osteoarthritis Cartilage.
432   2010;18:S24-S34.

433   17.   Guilak F, Ratcliffe A, Lane N, Rosenwasser MP, Mow VC. Mechanical and biochemical changes
434   in the superficial zone of articular cartilage in canine experimental osteoarthritis. J Orthop Res.
435   1994;12(4):474-484.

436   18.   Hollander AP, Pidoux I, Reiner A, et al. Damage to type II collagen in aging and osteoarthritis
437   starts at the articular surface, originates around chondrocytes, and extends into the cartilage with
438   progressive degeneration. J Clin Invest. 1995;96(6):2859-2869.

439   19.   Jackson MT, Moradi B, Zaki S, et al. Depletion of protease□activated receptor 2 but not
440   protease□activated receptor 1 may confer protection against osteoarthritis in mice through
441   extracartilaginous mechanisms. Arthritis Rheumatol. 2014;66(12):3337-3348.

442   20.   Jarvela T, Paakkala T, Kannus P, Jarvinen M. The incidence of patellofemoral osteoarthritis and
443   associated findings 7 years after anterior cruciate ligament reconstruction with bone-patellar tendon-bone
444   autograft. Am J Sports Med. 2001;29(1):18-24.

445   21.   Kroker A, Besler BA, Bhatla JL, et al. Longitudinal Effects of Acute Anterior Cruciate Ligament
446   Tears on Peri-Articular Bone in Human Knees Within the First Year of Injury. J Orthop Res.
447   2019;37(11):2325-2336.

448   22.   Kroker A, Bhatla JL, Emery CA, Manske SL, Boyd SK. Subchondral bone microarchitecture in
449   ACL reconstructed knees of young women: A comparison with contralateral and uninjured control knees.
450   Bone. 2018;111:1-8.

451   23.   Record #57 is using an undefined reference type. If you are sure you are using the correct
452   reference type, the template for that type will need to be set up in this output style.

453   24.   Lohmander LS, Ostenberg A, Englund M, Roos H. High prevalence of knee osteoarthritis, pain,
454   and functional limitations in female soccer players twelve years after anterior cruciate ligament injury.
455   Arthritis Rheum. 2004;50(10):3145-3152.

456   25.   Maerz T, Kurdziel M, Newton MD, et al. Subchondral and epiphyseal bone remodeling following
457   surgical transection and noninvasive rupture of the anterior cruciate ligament as models of post-traumatic
458   osteoarthritis. Osteoarthritis Cartilage. 2016;24(4):698-708.

459   26.   Maerz T, Kurdziel MD, Davidson AA, et al. Biomechanical characterization of a model of
460   noninvasive, traumatic anterior cruciate ligament injury in the rat. Ann Biomed Eng. 2015;43(10):2467-
461   2476.

462   27.   Maerz T, Newton M, Matthew H, Baker K. Surface roughness and thickness analysis of contrast-
463   enhanced articular cartilage using mesh parameterization. Osteoarthritis Cartilage. 2016;24(2):290-298.

464   28.   Maerz T, Newton MD, Fleischer M, et al. Traumatic joint injury induces acute catabolic bone
465   turnover concurrent with articular cartilage damage in a rat model of posttraumatic osteoarthritis. J
466   Orthop Res. 2020.

467   29.   Maerz T, Newton MD, Kurdziel MD, et al. Articular cartilage degeneration following anterior
468   cruciate ligament injury: a comparison of surgical transection and noninvasive rupture as preclinical
469   models of post-traumatic osteoarthritis. Osteoarthritis Cartilage. 2016;24(11):1918-1927.

470   30.   Mapp P, Sagar D, Ashraf S, et al. Differences in structural and pain phenotypes in the sodium
471   monoiodoacetate and meniscal transection models of osteoarthritis. Osteoarthritis Cartilage.
472   2013;21(9):1336-1345.

473   31.   McErlain D, Appleton C, Litchfield R, et al. Study of subchondral bone adaptations in a rodent
474   surgical model of OA using in vivo micro-computed tomography. Osteoarthritis Cartilage.
475   2008;16(4):458-469.

476   32.   Neuman P, Kostogiannis I, Fridén T, et al. Patellofemoral osteoarthritis 15 years after anterior
477   cruciate ligament injury–a prospective cohort study. Osteoarthritis Cartilage. 2009;17(3):284-290.

478   33.   Newton MD, Junginger L, Maerz T. Automated MicroCT-based bone and articular cartilage
479   analysis using iterative shape averaging and atlas-based registration. Bone. 2020:115417.

480   34.   Oiestad BE, Holm I, Engebretsen L, et al. The prevalence of patellofemoral osteoarthritis 12
481   years after anterior cruciate ligament reconstruction. Knee Surg Sports Traumatol Arthrosc.
482   2013;21(4):942-949.

483   35.   Owusu-Akyaw KA, Heckelman LN, Cutcliffe HC, et al. A comparison of patellofemoral cartilage
484   morphology and deformation in anterior cruciate ligament deficient versus uninjured knees. J Biomech.
485   2018;67:78-83.

486   36.   Palmer AW, Guldberg RE, Levenston ME. Analysis of cartilage matrix fixed charge density and
487   three-dimensional morphology via contrast-enhanced microcomputed tomography. Proc Natl Acad Sci U
488   S A. 2006;103(51):19255-19260.

489   37.   Potter HG, Jain SK, Ma Y, et al. Cartilage injury after acute, isolated anterior cruciate ligament
490   tear: immediate and longitudinal effect with clinical/MRI follow-up. Am J Sports Med. 2012;40(2):276-
491   285.

492   38.   Ramme A, Lendhey M, Raya J, Kirsch T, Kennedy O. A novel rat model for subchondral
493   microdamage in acute knee injury: a potential mechanism in post-traumatic osteoarthritis. Osteoarthritis
494   Cartilage. 2016;24(10):1776-1785.

495   39.   Stoop R, Buma P, van der Kraan PM, et al. Type II collagen degradation in articular cartilage
496   fibrillation after anterior cruciate ligament transection in rats. Osteoarthritis Cartilage. 2001;9(4):308-315.

497   40.   Tsai PH, Lee HS, Siow TY, et al. Abnormal perfusion in patellofemoral subchondral bone
498   marrow in the rat anterior cruciate ligament transection model of post-traumatic osteoarthritis: a dynamic
499   contrast-enhanced magnetic resonance imaging study. Osteoarthritis Cartilage. 2016;24(1):129-133.

500   41.   van Meer BL, Waarsing JH, van Eijsden WA, et al. Bone mineral density changes in the knee
501   following anterior cruciate ligament rupture. Osteoarthritis Cartilage. 2014;22(1):154-161.

502